

# Dark Confinement-Deconfinement Phase Transition: A Roadmap from Polyakov Loop Models to Gravitational Waves

Zhaofeng Kang,<sup>1,\*</sup> Shinya Matsuzaki,<sup>2,†</sup> and Jiang Zhu<sup>1,‡</sup>

<sup>1</sup>*School of physics, Huazhong University of Science and Technology, Wuhan 430074, China*

<sup>2</sup>*Center for Theoretical Physics and College of Physics, Jilin University, Changchun, 130012, China.*

(Dated: March 17, 2022)

We explore the confinement-deconfinement phase transition (PT) of the first order (FO) arising in  $SU(N)$  pure Yang-Mills theory, based on Polyakov loop models (PLMs), in light of the induced gravitational wave (GW) spectra. We demonstrate that the PLMs with the Haar measure term, involving models successful in QCD with  $N = 3$ , are potentially incompatible with the large  $N$  scaling for the thermodynamical quantities and the latent heat at around the criticality of the FOPT reported from the lattice simulations. We then propose a couple of models of polynomial form, which we call the 4-6 PLM (with four- and six-point interactions among the basic PL fields which have center charge 1) and 4-8 PLM (with four- and eight-point interactions), and discuss how such models can naturally arise in the presence of a heavy PL with charge 2. We show that those models give the consistent thermodynamical and large  $N$  properties at around the criticality. The predicted GW spectra are shown to have high enough sensitivity to be probed in the future prospected interferometers such as BBO and DECIGO.

## I. INTRODUCTION

Pure Yang-Mills (PYM) sector surviving at low energy is of particular interest in the new physics domain, because it is predicted in many contexts, such as dark matter/radiation [1–3], origin of baryon asymmetry [4], naturalness problem [5], and also in the string theory [6]. However, if such a PYM sector is sufficiently secluded from the visible sector, then what is its detectable signal?

Due to the asymptotic freedom of non-Abelian gauge theory, the PYM theory in the ultraviolet scale lies in the deconfinement phase described by free glues, whereas flowing to the infrared scale, the interactions between glues steadily get strong and eventually confine them to the colourless glueballs<sup>1</sup>. Therefore, there is a confinement-deconfinement transition at the critical temperature  $T_c$ . It is well-known that for the  $SU(N)$  PYM theory with  $N > 2$ , this phase transition (PT) is first order (FO). Then, one expects the corresponding first order cosmic/thermal PT in the early universe, during which gravitational waves (GW) are produced. They immediately decouple from the matters and are wandering in the universe today, which may meet the GW detectors in the sky such as the LISA [8, 9], Big Bang Observer (BBO) [10–14], DECIGO [14–16] and TianQin [17], where the sensitivities of frequencies cover a wide region from  $10^{-3}$  mHz to kHz; and the sensitivities can be improved in orders of magnitude over the next three decades.

To quantify the GW prediction, a phenomenological model of Ginzburg-Landau type modeling the confinement-deconfinement PT is useful. Nevertheless, a model commonly used lacks despite of many exploration along different lines. The reason is owing to the fact that the transition probably is the interplay of the perturbative and non-perturbative dynamics of the PYM theory. Lattice simulation, which presents the equilibrium thermodynamic properties of the  $SU(N)$  plasma at finite  $T$ , in particular for  $N > 3$  [18, 23], gives us important clues to construct effective models. The pressure  $p(T)$  is directly related to the potential of the model in terms of some fundamental degrees of freedom such as the Polyakov loop (PL) [24], thus of special importance:

- The pressure is found to scale as the ideal Stefan-Boltzmann (SB) limit when  $T > 4T_c$ , namely  $p(T) \sim (N^2 - 1)T^4$ . On the contrary, the pressure tends to vanish below  $T_c$ .
- A feature is observed by Meisinger and Pisarski etc [19, 21]<sup>2</sup>: The conformal anomaly  $\Delta(T)$ , the energy density  $\epsilon(T)$  minus  $3p(T)$ , is nearly a constant relative to the gluon gas limit within the semi-quark gluon plasma (sQGP)

---

\*E-mail: zhaofengkang@gmail.com

†E-mail: synya@jlu.edu.cn

‡E-mail: jackpotzhujiang@gmail.com

<sup>1</sup> These objects may be stable or sufficiently long-lived, providing a good candidate for the feebly interacting massive particle dark matter [7]. In that case, glueball decays and may leave detectable signals in the cosmic rays.

<sup>2</sup> It is first based on the precise data for three color [22, 23], but similar feature is also shown for other colors [25, 26]

region  $1.2T_c < T < 4T_c$ . This suggests that the non-perturbative correction may scale as  $T^2$ , and consequently in the sQGP region the pressure takes the form of

$$p(T) = c_1(T^4 - c_2 T_c^2 T^2), \quad (1)$$

with  $c_2 \simeq 1$ . The first term is supposed to be obtained after integrating out the hard modes at  $\mathcal{O}(T)$  in the weak-coupling expansion, recovering the ideal gluon gas limit indicated above. In terms of the PL,  $c_1$  is determined by the perturbative Weiss potential at leading order [27]. But to properly fit lattice data from  $T_c$  to  $1.2T_c$ , it is found that other terms such as the linear term  $T_c^3 T$  becomes important. Without a convincing theory to justify Eq. (1) in the whole region of  $T > T_c$ , one should keep an open mind. And we will come back to this point in the text.

Besides, the latent heat released during the FOPT shows a simple scaling behavior, i.e.,  $L_N \approx 0.388(N^2 - 1)T_c^4$  [18, 23]. Then, following the Polyakov Loop Model (PLM), one should find an effective potential of the PL encoding these features.

To this end, first of all, the potential of the PLM at hand should realize a FOPT, which severely limits the profile of the potential. To our knowledge, there are several types of PLM available which give rise to the FOPT supported from the lattice simulations. One type makes the FOPT triggered by the Haar measure term (the Vandermonde determinant interaction term) associated with the  $SU(N)$  group integral over the Polyakov loop variable [28]. Including a quadratic term of the PL variable (corresponding to the nearest-neighbor kinetic interaction term [28]), this Haar measure approach is shown to be consistent with the picture of ghost dominance in the infrared regime <sup>3</sup>, and is indeed successful in the case of QCD with  $N = 3$  and even with quarks. We shall label this approach as “Haar-type”. Based on this Haar measure prescription, Ref. [29] investigated a dark  $SU(N)$  gauge theory with colored scalars (in a scale-invariant setup) and the FOPT for the confinement-deconfinement, and discussed the related GW signals. However, the Haar measure term will be almost impossible to handle as  $N$  becomes large. Moreover, as will be clarified in the present paper, this Haar-type model turns out to have the incompatibility with the lattice data for  $N = 4, 5, 6$  in addressing the large  $N$  scaling for the thermodynamical quantities at around  $T = T_c$ .

As another approach, there is what is called the matrix model, motivated by the form of the Weiss potential [19]. This model treats the eigenvalues of the PL as variables [19, 30], where the FOPT is understood by the mutual repulsion of these eigenvalues. Unlike the previous models, this approach instead just utilizes the trace part of the PL, which is obviously gauge invariant, to construct the PLM [31, 32]. Very recently, Ref. [33] appeared which studies GWs from the PYM sector following the matrix-model approach <sup>4</sup>.

Though there are several models in the ballpark, it is still unclear how to realize the FOPT of the confinement-deconfinement for a generic  $N$ , consistently with the large  $N$ -thermodynamical feature relevant to the GW spectral predictions. In this paper, we explore  $SU(N)$  PLMs which can fully be consistent with the large  $N$  scaling for the thermodynamical quantities at around the criticality of the confinement-deconfinement PT, including the aforementioned thermodynamical properties above, hence can provide the proper GW spectral signals today. We demonstrate that the Haar-type model is potentially incompatible with those critical large  $N$  scaling properties reported from the lattice simulations.

We then propose a couple of simple-minded polynomial models, which we call the 4-6 PLM (having four- and -six point interaction terms) and 4-8 PLM (with four- and -eight point interaction terms), based on the spirit outlined in the literature [34] long ago. We show that the 4-6 and 4-8 PLMs can fully be consistent with the required thermodynamical and large  $N$  properties.

Actually, those PLMs are not completely novel, but have not received sufficient attention yet. The present work provides the derivation of the 4-6 PLM as well as the 4-8 PLM, and for the first time thoroughly analyzes the models, in light of GW spectra taking into account the consistency with the large  $N$  scaling coupled to the criticality of the confinement-deconfinement FOPT. We show that the predicted GW spectra can have high enough sensitivity to be probed in the future prospected interferometers such as BBO and DECIGO.

The paper is organized as follows: In Section II we start with a review of the generic ingredients to construct the PLMs including the  $Z_N$  center symmetry, the order parameter of the confinement-deconfinement PT, and introduction of a nonminimally- $Z_N$ charged PL variable (part A). With these preliminaries at hand, we employ a widely used conventional PLM, called the Haar-type PLM, and show that the model turns out to have incompatibility in a sense

<sup>3</sup> Ghost dominance is the Kugo-Ojima scenario of confinement, realized by the non-perturbative propagators of the ghost and the gluons [35, 36], leading to the inverted Weiss potential.

<sup>4</sup> We will not cover this approach in the present paper, but just give some comments on comparison in the last section, and will leave deeper relationship with what we will propose in another publication.

of the large  $N$  scaling for the latent heat and the other thermodynamical quantities at around the criticality for the confinement-deconfinement PT (part B). Then, we propose a set of PLMs which properly realizes the thermodynamical and the large  $N$  properties at around the criticality, that is what we call the 4-6 and 4-8 PLMs, with explanation on the derivation for those highly nonminimal coupling terms. The models are shown to yield the good-fitness with the  $SU(N)$  lattice data on the thermodynamical quantities, as well as the latent heat, regarding the large  $N$  scaling around the criticality (part C).

In Sec.III, we move on to discussion on the generation mechanism of the GW spectra by the FOPT based on the 4-6 and 4-8 PLMs. The dark  $SU(N)$  PYM is assumed to be the secluded-dark gluonic plasma (part A). Passing discussion on a couple of the well-known GW sources (part B), we numerically evaluate the GW spectra, in comparison with the prospected GW detector sensitivities (part C). Our conclusion and several issues still left with us are presented in Sec.IV.

## II. ROAD TO A PROPER PLM

### A. PLs and $Z_N$ center symmetry

It is commonly believed that the PL [24] plays a center role in understanding the confinement-deconfinement PT in the PYM theory. At the given  $T$ , it is shown that when a immovable test quark is placed at the position  $\vec{x}$ , its color-averaged free energy  $F_q(\vec{x})$  can be expressed as  $e^{-F_q(\vec{x})/T} = \langle \text{tr}_c L(\vec{x}) \rangle$  with  $L(\vec{x})$  the thermal Wilson line at fixed spatial position  $\vec{x}$  extending in the temporal direction:

$$L(\vec{x}) = \mathcal{P} \exp \left[ ig \int_0^{1/T} dx_4 A_4(\vec{x}, x_4) \right], \quad (2)$$

where  $g$  denotes the PYM gauge coupling, and the line is closed due to periodicity of the gauge field  $A_\mu$  as a bosonic field:  $A_4(\vec{x}, x_4) = A_4(\vec{x}, x_4 + 1/T)$ . Here  $A_4 \equiv A_4^a t^a$  with  $t^a$  ( $a = 1, \dots, N^2 - 1$ ) being the generators of  $SU(N)$  in the fundamental representation. Under the local  $SU(N)$  transformation,  $L$  transforms as the adjoint representation. Therefore, taking trace in the color space, one obtains a gauge invariant operator

$$l(\vec{x}) = \frac{1}{N} \text{tr}_c L(\vec{x}), \quad (3)$$

just the quantity aforementioned before and known as the PL. Quantum mechanically,  $l(\vec{x})$  is a local operator, while classically it is a complex scalar field with field value bounded by one:  $|l(\vec{x})| \leq 1$ . Note that  $l(\vec{x})$  is dimensionless by construction, and one should make up it by some dimensionful quantity in addressing the cosmic/thermal evolution of the GWs; we will come back to this point in Sec. III (around Eq.(37)).

Due to the compactified temporal direction, gauge fields should respect the periodicity shown before, however, gauge transformations  $V(\vec{x}, x_4)$  can be non-periodic. Instead, to keep the PYM action gauge invariant, they are just required to satisfy the twisted boundary condition (the center twisted gauge transformations):  $V(\vec{x}, \beta) = \tilde{z}_k V(\vec{x}, 0)$ , where  $\tilde{z}_k = e^{i2k\pi/N}$  with  $k = 1, 2, \dots, N$  belonging to the discrete group  $\tilde{Z}_N$ ; the transformation satisfying the periodicity corresponds to  $k = N$ . In particular, the gauge transformation with respect only to  $x_4$

$$V_k(x_4) = (z_k)^{x_4/\beta} = e^{i2k\pi x_4/(N\beta)} 1_{N \times N} \quad (4)$$

obviously obeys the twisted boundary condition; it is dubbed the center symmetry [37] since it is simply the power of the elements of  $z_k = \tilde{z}_k 1_{N \times N} \in Z_N$ , the center of  $SU(N)$ . Under the action of  $V_k(x_4)$ ,  $l$  is not invariant and changes as  $l \rightarrow z_k l$  although the Euclidean action is invariant. In this sense,  $l$  is charged under the global center  $Z_N$ . Now, it is seen that the gauge invariant operator  $l$  can serve as a good order parameter of the confinement-deconfinement PT:

- If  $\langle \text{tr}_c L(\vec{x}) \rangle = 0$  and  $Z_N$  is not broken, then  $F_q \rightarrow \infty$  thus quarks are confined.
- If  $\langle \text{tr}_c L(\vec{x}) \rangle \neq 0$  and  $Z_N$  is broken, then  $F_q$  is finite thus quarks are deconfined.

The exact  $Z_N$  charge of  $l$  is not determined from the first principle, and one may specify its charge as 1 and dub the basic PL. Other traced PLs with different  $Z_N$  charged can be introduced though seldom used [34, 38].

$$l_2 = \frac{1}{N} \text{tr}(L^2) - l_1^2, \quad \dots \quad l_N = \frac{1}{N} \text{tr}(L^N) - l_1^2 - l_2^2 \dots - l_{N-1}^2 \quad (5)$$

where the subscripts denote the  $Z_N$  charge, with  $l_1$  being the basic PL and  $l_N$  a “quarkless-baryon” loop, which is color singlet [34, 38]. In constructing PLM incorporating additional PLs, the couplings among them are constrained by  $Z_N$ . But the higher  $Z_N$  charged PLs are assumed to be heavy and can be integrated out, which leads to the polynomial potential we will use in Sec.II (See Eqs.(28) and (29), and discussions around there.).

## B. The Haar-type PLMs for general $SU(N)$ theory

### 1. The models

The Haar-type PLM is constructed based on the two-parameter model proposed by Fukushima [28, 39] for QCD with  $N = 3$ . It contains the nearest-neighbor coupling among PLs, so-called the kinetic term for the traced PL  $l$ , and as well as the Haar measure term  $H_N[L]$  which is crucial to trigger the FOPT. The Haar measure incorporates  $(N - 2)$  degrees of freedom other than  $l$ , which causes the complexity for a larger  $N$ . In the Polyakov gauge where  $A_4$  is diagonal,

$$A_4(\vec{x}) = \frac{2\pi}{g\beta} \text{diag}(q_1(\vec{x}), q_2(\vec{x}), \dots, q_N(\vec{x})) \quad (6)$$

with  $\sum_i q_i = 0$ , then  $H_N[L]$  is given by

$$H_N[L(\vec{x})] = \prod_{i < j} |e^{i2\pi q_i(\vec{x})} - e^{i2\pi q_j(\vec{x})}|^2. \quad (7)$$

The Haar-type PLM, generalized from the original model for  $N = 3$  [28, 39] to any color [29], thus goes like

$$\frac{V(L, T)_{\text{Haar},0}}{T^4} = \mathcal{V}_{\text{Haar},0}(L, T) = b_N [6 \exp(-a/T) l l^\dagger + \log H_N[L]], \quad (8)$$

where the form of the kinetic term has been fixed inspired by the strong coupling expansion;  $a$  and  $b_N$  are two parameters needed to be determined by lattice data. Although it successfully explains the confinement-deconfinement PT of the first order, it can not reproduce the observed thermodynamics in lattice simulation, as will be clarified later.

Soon later we will show that it is true even in another Haar-type PLM (for  $N = 3$ ) studied in Ref. [40], which has a kinetic term including more parameters, generalized to any color number:

$$\begin{aligned} \mathcal{V}(L, T)_{\text{Haar},1} &= -\frac{a(T)}{2} l l^\dagger + b(T) \log H_N[L], \\ a(T) &= a_0 + a_1 \left(\frac{T_c}{T}\right) + a_2 \left(\frac{T_c}{T}\right)^2 \quad b(T) = b_3 \left(\frac{T_c}{T}\right)^3. \end{aligned} \quad (9)$$

The potential parameters  $a_0, a_1, a_2$  and  $b_3$  are constrained and fixed by imposing some physical conditions and fitting this potential to the lattice data on the thermodynamical quantities.

### 2. Constraining the potential parameters from first-order deconfinement PT

As to the required thermodynamical constraints, there are two. One is set by requiring that as noted in the Introduction, at high temperature the PL potential should realize the SB limit in the deconfinement vacuum  $l = l_c$ , which must go to 1 as  $T \rightarrow \infty$  (because in this limit  $L \rightarrow 1$  by definition, see Eq. (2)) and therefore  $T^4 \mathcal{V}(T) = -\frac{(N^2-1)\pi^2}{45} T^4$ . It fixes  $a_0$ :

$$a_0 = \frac{2(N^2 - 1)\pi^2}{45}. \quad (10)$$

The other condition is given by assuming that the FOPT takes place at the critical temperature  $T_c$ , namely that two minima should be degenerate at  $T = T_c$ . This condition gives a set of equations

$$\begin{aligned} \mathcal{V}(L_c, T_c) &= \mathcal{V}(L_0, T_c), \\ \left. \frac{\partial \mathcal{V}(L, T)}{\partial L} \right|_{L=L_c, T=T_c} &= 0, \\ \left. \frac{\partial \mathcal{V}(L, T)}{\partial L} \right|_{L=L_0, T=T_c} &= 0, \end{aligned} \quad (11)$$

where the labels  $c$  and  $0$  attached on the  $L$ s respectively stand for the values measured in the deconfinement phase ( $T > T_c$ ) and the confinement phase ( $T < T_c$ ). The last condition in Eq.(11) gives the stationary point in the confinement phase, which has to be realized at  $L_0 = l_0 = 0$  so as to reflect the  $Z_N$  center symmetry in the confinement phase. Note from the potential form in Eq.(9) that this condition is controlled solely by the Haar measure term, no matter what values independent of the potential parameters  $a_0, a_1, a_2, b_3$  take. The remaining first two conditions in Eq. (11) read

$$\begin{aligned} -\frac{a_0 + a_1 + a_2}{2} l_c l_c^\dagger + b_3 \log H_N(L_c) &= b_3 \log H_N(L_0), \\ -(a_0 + a_1 + a_2) l_c + \frac{b_3}{H_N(L_c)} \frac{\partial H_N(L_c)}{\partial l_c} &= 0, \end{aligned} \quad (12)$$

i.e.,

$$\begin{aligned} b_3 &= l_c \frac{H_N(L_c)}{\frac{\partial H_N(L_c)}{\partial l_c}} (a_0 + a_1 + a_2), \\ -\frac{l_c^\dagger}{H_N(L_c)} \frac{\partial H_N(L_c)}{\partial l_c} + 2 \log H_N(L_c) &= 2 \log H_N(L_0). \end{aligned} \quad (13)$$

Thus, given the Haar measure term  $H_N$ , the field value  $l_c$  can be numerically determined by solving the second relation in Eq.(13), as is independent of the potential parameters. With  $l_c$ , we combine the first and second relations in Eq.(13), and obtain the relation between the potential parameters

$$b_3 = -\frac{l_c^\dagger l_c}{2} \frac{1}{\log[H_N(L_0)/H_N(L_c)]} (a_0 + a_1 + a_2). \quad (14)$$

### 3. Fitting the potential parameters from thermodynamics

The potential parameters should also be fitted to the thermodynamical quantities measured in lattice simulations, such as pressure  $P$ , energy density  $\epsilon$  and the entropy density  $s$ . From the potential in Eq.(9), those thermodynamical quantities can be evaluated as

$$\begin{aligned} P(T) &= -V(T), \\ \epsilon(T) &= \frac{dU(T)}{dV} = T \frac{dS(T)}{dV} - P(T) = T \frac{dP(T)}{dT} - P(T), \\ s(T) &= \frac{dS(T)}{dV} = \frac{P(T) + \epsilon(T)}{T}. \end{aligned} \quad (15)$$

In light of GW signals, of particular importance among the thermodynamical properties is the latent heat for the confinement-deconfinement PT of the first order. Given the PL potential as in Eq.(9), the latent heat  $L_N$  for  $SU(N)$  PYM theory is defined as

$$L_N(T_c) = -\Delta V(T_c) + T \left. \frac{\partial \Delta V(T)}{\partial T} \right|_{T=T_c}, \quad (16)$$

where  $\Delta V(T) = V(L_0, T) - V(L_c, T)$ . Taking into account the first relation in Eq.(11), we have

$$\begin{aligned} L_N &= T_c \left. \frac{dV(L_0, T)}{dT} \right|_{T=T_c} - T_c \left. \frac{dV(L_c, T)}{dT} \right|_{T=T_c} \\ &= T_c^4 \left[ (4a_0 + 3a_1 + 2a_2) \frac{l_c l_c^\dagger}{2} + b_3 \log \frac{H_N(L_0)}{H_N(L_c)} \right]. \end{aligned} \quad (17)$$

To this  $L_N$ , lattice simulations tell us [18, 23]

$$\frac{L_N}{(N^2 - 1)T_c^4} \simeq 0.388 - \frac{1.61}{N^2}, \quad (18)$$

which implies

$$\log \left[ \frac{H_N(L_0)}{H_N(L_c)} \right] \cdot b_3 \simeq (N^2 - 1) \left( 0.388 - \frac{1.61}{N^2} \right) - \frac{l_c l_c^\dagger}{2} (4a_0 + 3a_1 + 2a_2). \quad (19)$$

This is the potential parameter relation for the Haar-type PLM, which must be satisfied to be consistent with the vicinity of the FOPT in the  $SU(N)$  PYM theory. Actually, using  $b_3$  given in Eq. (14), the above equation turns out to be a relation among  $a_i$ :

$$\frac{l_c l_c^\dagger}{2} (3a_0 + 2a_1 + a_2) \simeq (N^2 - 1) \left( 0.388 - \frac{1.61}{N^2} \right), \quad (20)$$

where  $a_0$  has been fixed as in Eq.(10).

It turns out, however, that the potential parameters in the Haar-type PLMs are inconsistent with the lattice data on thermodynamical quantities in  $SU(N)$  gauge theory, in terms of the large  $N$  scaling. We come to this conclusion with great help from the work of Kubo [29], and let us explain the details in the following.

#### 4. No Go in a View of Large $N$ Scaling and the $SU(N)$ PYM criticality

From the numerical result [29] that no matter how large  $N$  is taken,  $l_c$  is found to be around 0.5. Taking into account this result and  $a_0 = \frac{2(N^2-1)\pi^2}{45}$  in Eq.(10), we have

$$\frac{1}{8} (2a_1 + a_2) \simeq (N^2 - 1) \left( 0.224 - \frac{1.61}{N^2} \right) \quad (21)$$

Thus the parameters  $a_0, a_1$  and  $a_2$  can scale with  $(N^2 - 1)$  for a sufficiently large  $N$ . On the contrary, actually, the parameter  $b_3$  cannot do because of nontrivial  $N$  dependence of the Haar measure part present as a prefactor in Eq.(14). As references, we know [29] that  $H_3(L_0)/H_3(L_c) \sim 0.9$ ,  $H_4(L_0)/H_4(L_c) \sim 2.6$ ,  $H_5(L_0)/H_5(L_c) \sim 4.8$  and  $H_6(L_0)/H_6(L_c) \sim 12.7$ , which implies

$$\frac{\log[H_{N_1}(L_0)/H_{N_1}(L_c)]}{\log[H_{N_2}(L_0)/H_{N_2}(L_c)]} > \frac{N_1^2 - 1}{N_2^2 - 1}, \quad (22)$$

for large enough  $N_1$  and  $N_2$ . Therefore, the parameter  $b_3$  cannot simply scale with  $(N^2 - 1)$ . This is in contradiction with the lattice result [41] showing the universal large  $N$  scaling for all thermal quantities  $\propto (N^2 - 1)$ , which indicates that all Polyakov loop potential parameters should be proportional to  $N^2 - 1$  as well. This incompatibility arises from the Haar measure part included in the potential, driving the nontrivial  $N$  dependence into the thermodynamics in  $SU(N)$  gauge theory.

As a concrete example, let us take a look at the case with  $N = 4$ . Then we have

$$\log \frac{H_4(L_0)}{H_4(L_c)} \simeq 2.5562. \quad (23)$$

Hence Eq. (19) reads

$$2.5562 \times b_3 \simeq 4.311 - 0.1247 \times (4a_0 + 3a_1 + 2a_2). \quad (24)$$

On the other hand, from Eq.(14), we have

$$b_3 \simeq -0.0488(a_0 + a_1 + a_2). \quad (25)$$

Combining them gives

$$a_2 \simeq 34.5562 - (3a_0 + 2a_1). \quad (26)$$

Substituting these conditions into the fitting program for the thermodynamical quantities in  $SU(4)$  gauge theory, with data available from [41], we have found the fit does not match the lattice result at all <sup>5</sup>.

Thus, it is concluded that the Haar type PL potential in Eq.(9) for generic  $SU(N)$  gauge theory possesses incompatibility between the latent heat, i.e., confinement-deconfinement phase transition feature, and the overall large  $N$  scaling for the thermodynamical quantities.

### C. A Proper Model: Polynomial Potential

#### 1. The 4-6 PLM versus 4-8 model

Now that we have demonstrated the Haar type PLM in Eq.(9) to have incompatibility between the latent heat nature of the FOPT and the large  $N$  scaling, we need to consider other PLMs. For  $N = 3$ , there is a very successful potential structure of polynomial form with powers of  $l$  not exceeding 4 (renormalizability) [42], where the FOPT is triggered by the well-known cubic term  $(l^3 + l^{*3})$  by virtue of the underlying  $Z_3$  [37]. Nevertheless, this minimal polynomial form obviously fails for a generic  $Z_N$ . On the other hand, the large  $N$  scaling property revealed by lattice data strongly indicates that there must be a simple way to construct the PLM, irrespective of  $N$  not less than 3.

Thus we propose a simple PLM containing three terms,

$$\mathcal{U}(l, T) = \frac{V(l, T)}{T^4} = -\frac{a(T)}{2}|l|^2 + b|l|^4 + c|l|^6, \quad (27)$$

It is noticed that the terms in Eq. (27) are allowed by any  $Z_N$  symmetry, and actually they are consistent with a global  $U(1)$  symmetry. Although this PLM applies to  $N = 3$ , which has a weak FOPT, our focus is the case  $N > 3$ . We ignore the roles of other terms that may be allowed by  $Z_N$ , for instance  $l^4 + l^{*4}$  for  $N = 4$ , and so on. Such a treatment is to understand the large  $N$  scaling property in a unified way.

Comments on the potential parameters are in orders. It is assumed that  $a(T) = a_0 + a_1(\frac{T_c}{T}) + a_2(\frac{T_c}{T})^2 + a_3(\frac{T_c}{T})^3$  as usual, but other couplings are  $T$ -independent. In order to fit the sQGP region  $1.2T_c < T < 4T_c$ , the pressure may take the simple form shown in Eq. (1), and consequently the  $a_1$ -term namely the  $T^3$  term (in terms of the potential  $V(l, T)$ ) is not important while the  $a_2$ -term is important. However, the  $a_3$ -term namely the  $T$  term is crucial to fit the region very close to  $T_c$ , which will be confirmed by fitting to the lattice data later (See Figs. 1, 3 and Table I). A different viewpoint has been proposed by Fukushima in Ref. [39]: The PL potential is merely dominant to the contributions to the pressure of the system below about  $2T_c$ , and it should give way to the transverse gluons at the higher temperature; therefore, the PLM giving a pressure below the lattice data for  $T \gtrsim 2T_c$  is acceptable. We will investigate both scenarios (with or without  $a_2$ ) in the lattice fitting procedure, to find that, as expected, they are almost “degenerate” PLMs in a view of the GW signals (See Fig. 7).

Our PLM is characterized by two features: 1) The quartic term with a negative sign  $b < 0$ ; 2) a nonrenormalizable term with a positive sign  $c > 0$  to stabilize the potential. These two terms create the deconfined vacuum at  $l \neq 0$ . In the mean field theory, the nonrenormalizable terms usually are not taken into account, but its legitimacy, along with the sign of the quartic term, may be justified in the presence of additional and non-minimally charged PLs defined in Eq. (5). This potential form frees from extra large  $N$  scaling, other than the overall factor of  $(N^2 - 1)$  for all the potential parameters at around the  $SU(N)$  gauge criticality, as will be clearly seen below.

Let us briefly explain how the 4-6 structure of the PLM in Eq.(27) can arise following the spirit of Pisarski outlined in Ref. [34]. The key is the presence of charge-two PL,  $l_2$ , which always allows a cubic coupling with the basic PL,  $l$ , like  $l^2 l_2^*$ . The most general two-field model is given by

$$\mathcal{U}(l, l_2) \supset m_2^2 |l_2|^2 + m^2 |l|^2 + [\lambda_1 (ll^*)^2 + \lambda_2 (l_2 l_2^*)^2 + \lambda_{12} |l|^2 |l_2|^2] + a_{12} (l^2 l_2^* + c.c.), \quad (28)$$

---

<sup>5</sup> We have checked that this failure will not be cured even removing the SB limit condition in Eq.(10) which has not well been reproduced in lattice simulations somehow.

with taking  $a_{12}$  to be real. Assuming  $m_2$  heavy while  $m$  light around  $T_c$ , then  $l_2$  can be integrated out. Among others, this procedure produces a four-point interactions  $|l_1|^4$  with a negative coupling  $-a_{12}^2/m_2^2 \equiv -\tilde{\lambda}_2 < 0$ . The negativeness of the induced quartic coupling is robust, because, in terms of the  $ll \rightarrow ll$  scattering process, it arises from the  $l_2$ -scalar exchange involving the trilinear  $a_{12}$  interaction, which gives rise to the repulsive potential for the two  $l$  probes (in the nonrelativistic limit). The total effective PLM below the  $m_2$  scale reads

$$\mathcal{U}(l)_{eff} \supset m^2 |l|^2 + \left( \lambda_1 - \tilde{\lambda}_2 \right) |l|^4 + \lambda_{12} \tilde{\lambda}_2^2 |l|^6 + \lambda_2 \tilde{\lambda}_2^2 |l|^8. \quad (29)$$

Hence, if the bare coupling  $\lambda_1$  is properly chosen to make  $\lambda_1 < \tilde{\lambda}_2$ , the total quartic coupling is naturally negative, triggering the FOPT. Moreover, when we turn off either  $\lambda_2$  or  $\lambda_{12}$  for simplicity or minimality, then the above model respectively gives rise to the 4-6 (as in Eq.(27)) or 4-8 structure as desired – which we shall call the 4-6 and 4-8 PLMs, respectively.

The case  $N = 2$  is an exception since the confinement-deconfinement PT becomes second order, which may be accidentally due to the smallness of  $\tilde{\lambda}_2$ . Actually, in this case  $l_2$  is the “quarkless-baryon” loop [34], which is a singlet thus supposed to develop the vacuum expectation value any temperature. This vacuum expectation value should be very small, otherwise it would contribute significantly to the pressure of the system, contradicting with the lattice data. This argument is applicable to any other quarkless-baryon loops.

## 2. Lattice fitting of the potential parameters in the 4-6 PLM

The potential parameters are constrained as follows. First, the trace of PL field ( $l$ ) needs to asymptotically get close to 1 when one approaches the classical limit where  $T \rightarrow \infty$ . This condition can be realized by taking

$$\left. \frac{\partial V(l, T \rightarrow \infty)}{\partial l} \right|_{l=1} = 0, \quad (30)$$

or assuming the SB limit value, as done in Eq.(10). The second condition comes from the FOPT nature, as in Eq.(11):

$$\begin{aligned} \mathcal{U}(l_0 = 0, T_c) &= \mathcal{U}(l_c, T_c) \\ \left. \frac{\partial \mathcal{U}(l, T_c)}{\partial l} \right|_{l=l_0=0} &= \left. \frac{\partial \mathcal{U}(l, T_c)}{\partial l} \right|_{l=l_c} = 0. \end{aligned} \quad (31)$$

We have particular interest in the vicinity of the confinement-deconfinement PT at  $T = T_c$  and consistency with the large  $N$  scaling for the thermodynamical quantities around there. In that case, it turns out that the parameters  $a_1$  and  $a_2$  are fairly insensitive to this FOPT criticality: Near the critical temperature  $T_c$ , the potential can be simplified as  $V = \frac{1}{2} \sum_{i=0}^3 a_i |l|^2 + b |l|^4 + c |l|^6$ , where among the parameters  $a_i$ , the  $a_3$  term is most dominant because of its lowest power contribution by  $T_c T$  around  $T = T_c$  in the potential. Hence the potential around  $T = T_c$  should be almost controlled by the  $a_3$  term, so should the pressure. Taking into account the classical limit satisfied by Eq.(30), we see that the  $a_0$  term is also relevant. Thereby, dropping the parameters  $a_1$  and  $a_2$ , we can safely work on the remaining relevant parameter space.

The relevant parameter space is then constrained by the conditions in Eqs.(30) and (31), together with the desired large  $N$  scaling of the latent heat in Eq.(18) along with Eq.(16), as follows:

$$\begin{aligned} 0 &= -a_0 + 4b + 6c, \\ |l_c|^2 &= \frac{-b + \sqrt{b^2 + 4(a_0 + a_3)c}}{2c}, \\ 0 &= -(a_0 + a_3) + 4b|l_c|^2 + 6c|l_c|^4, \\ (N^2 - 1) \left( 0.388 - \frac{1.61}{N^2} \right) &\simeq -\frac{3a_3}{2} |l_c|^2. \end{aligned} \quad (32)$$

Thus, all the potential parameters can scale with  $(N^2 - 1)$  in the large  $N$  limit, consistently with the lattice observation. Figure 1 shows the 4-6 PLM fits to the lattice  $SU(N)$  thermodynamics with data from [41], with focusing on the confinement-deconfinement FOPT at around  $T = T_c$ . The left panel has been drawn by assuming  $a_1 = a_2 = 0$ , while the right panel made with assuming nonzero  $a_2$ . Comparison of both panels indeed implies the insensitivity of  $a_1$  and



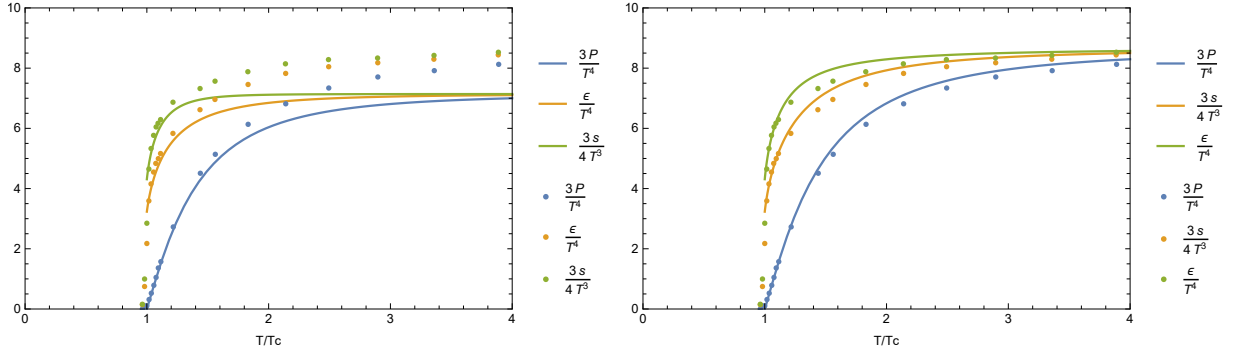


FIG. 1: Fitting the 4-6 PLM to the thermodynamical quantities of  $SU(4)$  PYM theory, observed in the lattice simulations [41], at around the critical temperature ( $T_c$ ) for the confinement-deconfinement phase transition of the first order. Left panel: Thermodynamical quantities as a function of  $T/T_c$  with the best fit parameters  $a_0 = 4.95$ ,  $a_1 = 0$ ,  $a_2 = 0$ ,  $a_3 = -6$ ,  $b = -2.19$  and  $c = 2.28$  for left panel, while those with  $a_0 = 6.36$ ,  $a_1 = 0.04$ ,  $a_2 = -2.68$ ,  $a_3 = -4.72$ ,  $b = -2.28$  and  $c = 2.58$  for right panel

$a_2$  to the thermodynamics around the criticality. See also Table I, which more precisely shows the best fit for the  $N = 4$  4-6 PLM without those parameters to the lattice data points.

Of importance is to note that the 4-6 PLM with  $N = 4$ , which has been fixed by fitting to the lattice data as above, can be used to construct another 4-6 PLM with  $N \geq 5$ : Given certain  $a_3$  for some  $SU(N)$  PLM, using the large  $N$  scaling  $a_3 \rightarrow \frac{M^2-1}{N^2-1}a_3$  from  $N$  to  $M$  and Eq. (32), one can immediately get a 4-6 PLM for  $SU(M)$ . This is possible because the last equation in Eq. (32) tells us that, in the large  $N$  limit, the parameter  $a_3$  is approximately proportional to  $N^2 - 1$  and other equations do not contain direct  $N$  dependence. Note also that the lattice data tell us thermal quantities  $\propto N^2 - 1$  and the large  $N$  scaling of the latent heat  $\approx N^2 - 1$ . Therefore, if  $N$  is large enough then the all relevant parameters for the  $SU(M)$  4-6 PLM should scale like

$$a_0 \rightarrow \frac{M^2-1}{N^2-1}a_0, \quad a_3 \rightarrow \frac{M^2-1}{N^2-1}a_3, \quad b \rightarrow \frac{M^2-1}{N^2-1}b, \quad c \rightarrow \frac{M^2-1}{N^2-1}c. \quad (33)$$

Figure 2 and Table I show how these scaling laws work for  $SU(5)$  and  $SU(6)$ , where the potential parameters have been scaled from the  $N = 4$  4-6 PLM as in Fig. 1 (and also the same Table I).

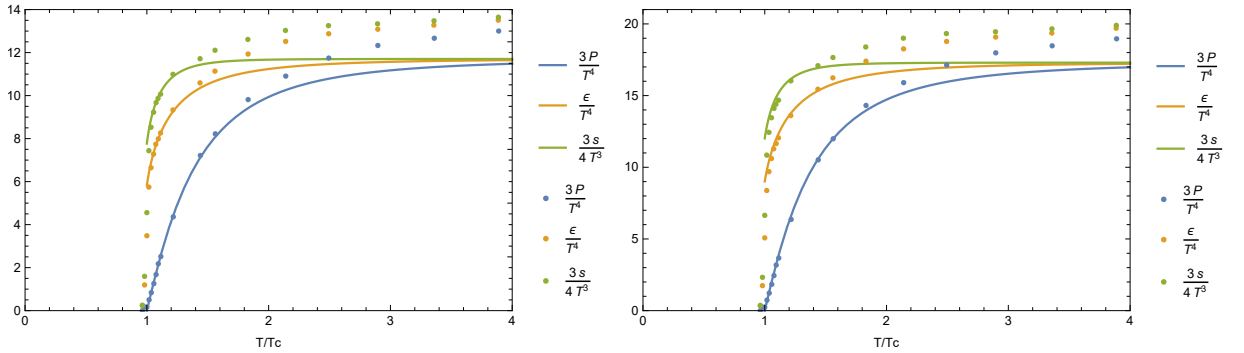


FIG. 2: Check on the large  $N$  scaling for the 4-6 PLM. Left panel: Fitting the 4-6 PLM for  $SU(5)$  to the thermodynamical quantities measured in the lattice simulation [41]. Right panel: The same for  $SU(6)$ . The lattice data for  $N = 5$  has been read off by using the large  $N$  scaling for the  $N = 6$  data in [41]. For both  $N = 5$  and  $N = 6$  cases, the potential parameters have been fixed by the large  $N$  scaling from the  $N = 4$  case in Fig. 1. See Table I for the values of the scaled parameters for  $SU(5)$  and  $SU(6)$  cases, and the goodness-of-fit.

Thus the large  $N$  scaling procedure allows us to save the fitting steps. However one may note from Table I that the goodness-of-fit has deteriorated with increasing  $N$ . This is because of the fact that the latent heat is merely approximately proportional to  $N^2 - 1$ , and for  $N = 4$  which is our reference model to start scaling, the large  $N$  subleading term ( $\frac{1.61}{N^2}$  in the last relation, in Eq.(32)) is actually comparable with the leading term (0.388 in the last, in Eq.(32)) hence cannot be ignored. The result will become better if the starting color number is bigger.

### 3. Lattice fitting of the potential parameters in the 4-8 PLM

Following the same method as done in discussing the 4-6 PLM above, we can analyze the 4-8 PLM. The potential parameter relation then takes the form similar to Eq. (32):

$$\begin{aligned}
0 &= -a_0 + 4b + 8c, \\
|l_c|^2 &= -\frac{2\left(\frac{2}{3}\right)^{1/3}b}{2\left(9(a_0 + a_3)c^2 + \sqrt{3}\sqrt{32b^3c^3 + 27(a_0 + a_3)^2c^4}\right)^{1/3}} \\
&\quad + \frac{\left(9(a_0 + a_3)c^2 + \sqrt{3}\sqrt{32b^3c^3 + 27(a_0 + a_3)^2c^4}\right)^{1/3}}{2^{4/3} \times 3^{2/3}c}, \\
0 &= -(a_0 + a_3) + b|l_c|^2 + c|l_c|^6, \\
(N^2 - 1)\left(0.388 - \frac{1.61}{N^2}\right) &\simeq -\frac{3a_3}{2}|l_c|^2.
\end{aligned} \tag{34}$$

Thus the 4-8 PLM can also realize the desired large  $N$  scaling for the thermodynamical quantities in  $SU(N)$  PYM theory consistently with the large  $N$  property of the latent heat. The result for fitting to the lattice data is shown in Fig. 3, and the best-fit parameters are listed in Table I.

Similarly to the 4-6 PLM, this 4-8 PLM can also create a set of a simple large  $N$  copies because of the manifest large  $N$  scaling: starting with the 4-8 PLM model having the color  $N$  with the potential parameters fixed, one can easily get the corresponding set of the potential parameters for another model with the color  $M$ , just by accessing the simple large  $N$  scaling:  $V \rightarrow \frac{M^2-1}{N^2-1}V$ , as in Eq.(33).

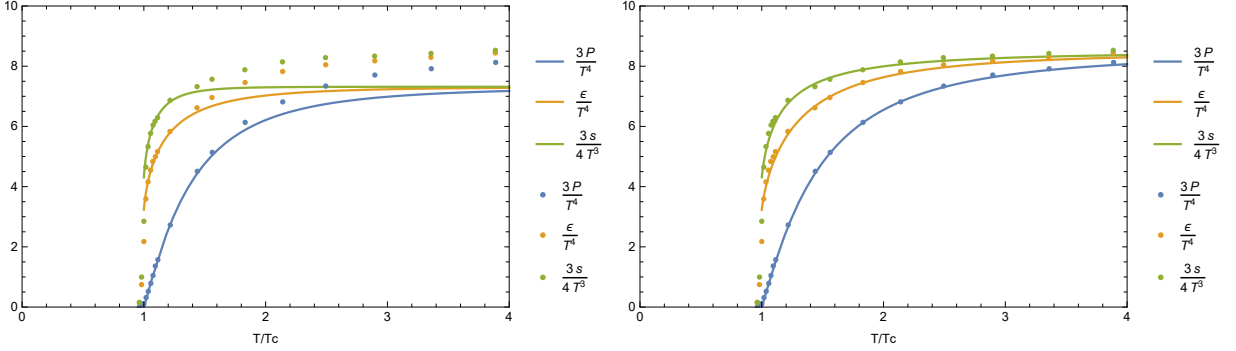


FIG. 3: Fitting the  $N = 4$  4-8 PLM to the thermodynamical quantities of  $SU(4)$  PYM theory. Left panel: Thermodynamical quantities as a function of  $T/T_c$  with the best fit parameters listed in Table I corresponding to the case  $N = 4_1$  for the 4-8 PLM. Right panel: The same for the case  $N = 4_2$  with the best-fit parameters in the list of the 4-8 PLM, in Table I.

## III. GW SPECTRA BASED ON THE 4-6 AND 4-8 PLMS

### A. Dark confinement-deconfinement FOPT in a secluded gluonic plasma

The GW associated with the confinement-deconfinement PT would be generated from the bubble nucleation of the confinement vacuum. The bubble nucleation rate per spacetime,  $\Gamma$ , contains two contributions. The first one comes from its thermal fluctuation,  $\Gamma(T)$ , and the second one generated by the quantum effects. In the present study, we ignore the second contribution because the quantum effects would dominate only in supercooling.

The thermal contribution to the bubble nucleation rate per volume per time is generically given by

$$\Gamma(T) \approx AT^4 e^{-\frac{S_3(T)}{T}}, \tag{35}$$

where  $A$  is supposed to be of  $\mathcal{O}(1)$ , and  $S_3(T)$  is the  $O(3)$  symmetric action in three-dimensional Euclidean space:

$$S_3(T) = 4\pi \int_0^\infty R^2 dR \left[ \frac{1}{2} \left( \frac{d\phi}{dR} \right)^2 + V(\phi, T) \right], \tag{36}$$

Parameter for 4-6 PLM							
Color number	$a_0$	$a_1$	$a_2$	$a_3$	$b$	$c$	$\chi^2/n$
$N = 4_1$	4.9522	0	0	-6	-2.1877	2.2839	0.166
$N = 4_2$	6.3599	0.0371	-2.6796	-4.7265	-2.2827	2.5818	0.320
$N = 5$	7.1365	0	0	-9.6	-4.5676	4.2345	0.085
$N = 6$	9.5886	0	0	-14.0	-7.7105	6.7385	0.438
$N = 7$	12.3551	0	0	-19.2	-11.5643	9.7687	1.385
$N = 8$	16.2160	0	0	-25.2	-15.1781	12.8214	2.224
Parameter for 4-8 PLM							
Color number	$a_0$	$a_1$	$a_2$	$a_3$	$b$	$c$	$\chi^2/n$
$N = 4_1$	5.54	0	0	-6	-0.7261	1.06	0.143
$N = 4_2$	6.24	0	-3.70	-3.2	-0.9794	1.27	0.103
$N = 5$	9.22	0	-5.75	-5.19	-2.25	2.28	0.067
$N = 6$	12.02	0	-8.42	-7.18	-4.29	3.65	0.183
$N = 7$	14.70	0	-11.71	-9.32	-7.15	5.41	0.475
$N = 8$	16.73	0	-16.29	-10.98	-11.33	7.76	0.912
$N = 9$	20.20	0	-20.69	-13.94	-15.29	10.17	1.810
$N = 10$	24.00	0	-25.60	-17.25	-19.78	12.89	3.222
$N = 11$	28.14	0	-31.02	-20.91	-24.77	15.90	5.288

TABLE I: The fitting parameters for the 4-6 and 4-8 PLMs. The two groups on the list for the case of  $N = 4$  separate two categories: one is the case where only  $a_3$  is used as the fitting parameter (corresponding to  $N = 4_1$ ), and the other case treats all  $a_1, a_2$ , and  $a_3$  as the fitting parameters ( $N = 4_2$ ). The  $n$  denotes the number of data and the  $\chi^2$  fits for the  $N = 4$  PLMs have been performed based on the data for  $T \leq 1.2T_c$ . As to the cases with  $N = 5$  and  $N \geq 7$ , which are directly unavailable from [41], the prospected data have been read off by using the large  $N$  scaling from  $N = 5$  or 6 data, and the fitting has been done by using the method described in the text. Therefore, their  $\chi^2/n$  values are relatively poorer, but showing still an acceptable goodness of fitting. This poorer fitness is due to the fact that the amplitudes of the thermal quantities increase with  $N$ , hence are quite hard to control, while the absolute error remain unchanged.

with  $R = |\vec{x}|$ .  $V(\phi, T)$  denotes an effective potential for two vacua (false vacuum and true vacuum), and  $\phi(R)$  is the bounce solution satisfying the Euclidean equation of motion

$$\frac{d^2\phi}{dR^2} + \frac{2}{R} \frac{d\phi}{dR} = V', \quad (37)$$

with  $V' \equiv \partial V(\phi, T)/\partial\phi$ , and the boundary conditions  $\lim_{R \rightarrow \infty} \phi(R) = 0$  (at the false vacuum position) and  $\frac{d\phi(R)}{dR}|_{R \rightarrow 0} = 0$ .

One thing to note is that the generic bounce solution has mass dimension 1, so that the exponent  $S_3(T)/T$  in Eq.(35) is dimensionless. On the contrary, in the PYM case, the role of the bounce solution is played by the trace of the PL field,  $l$ , which is dimensionless. To match the case with the generic thermal evolution in Eq.(35), we need to rescale  $l$  so as to have mass dimension 1, like  $l \rightarrow l/\Lambda$ , and fix the scale parameter as  $\Lambda = T$ . This scaling would be reasonable because  $l$ , or  $L$  in Eq.(2) involves only the temperature  $T$  as the dimensionful parameter. Similar prescription has been applied in the literature [38].

Another thing to note is the distinction between the temperatures of the dark gluonic bath and of the bath made of the standard model (SM) particles. We label them respectively as  $T$  (for the dark PYM sector) and  $\mathcal{T}$  (for the SM sector). By definition of PYM, which incorporates no matters, the two baths should decouple and thermalize individually. In  $\Gamma(T)$ , Eq.(35), the prefactor  $T^4$  originates from the space time volume evolved by the scale factor  $a$  of the universe as  $V = a^3 t$ , so should be identified simply with neither  $\mathcal{T}$  nor  $T$ . However, the difference in  $T$  and  $\mathcal{T}$  actually does not matter much since it merely gives a logarithmic correction to the nucleation temperature  $T_n$ . Whereas both temperatures in  $S_3(T)/T$  (the argument of  $S_3$  and the normalization factor for the exponential,  $1/T$ ) should be associated with the dark PYM-sector: In  $S_3(T)$ ,  $T$  is supplied from a given PLM, and the origin of  $1/T$  is traced back to the imaginary-time formalism in the thermal field theory, where  $T$  should be the temperature of the thermal bath created in the thermalized dark PYM.

In the temperature region of interest (say, before the big-bang nucleosynthesis (BBN)) where both baths are in the form of radiation <sup>6</sup>, then  $T_i = \left(\frac{30\rho_i}{\pi^2} g_i^*\right)^{1/4}$  with  $T_1 = T$  and  $T_2 = \mathcal{T}$ , and similar for others. Here  $\rho_i$  and  $g_i^*$

<sup>6</sup> This is imprecise for the dark gluonic sector when it enters the sQGP region and further approaches the transition, where the equation of matter deviates from radiation more and more significantly. But our discussions approximately hold as long as the universe is not dominated by the PYM sector.

are the energy density and relativistic degrees of freedom in the bath, respectively. Further assuming that entropy is conserved, then both temperatures scale as  $1/a$ , which is expanding with the Hubble parameter

$$H = \sqrt{(\rho_{\text{SM}} + \rho_{\text{PYM}}) / 3M_{\text{Pl}}^2}. \quad (38)$$

As a consequence, in the thermal epoch under consideration, the ratio  $\zeta \equiv \mathcal{T}/T$  keeps a constant, determined by the production mechanism of the two sectors. To the end of correct relic density of dark glueball dark matter,  $\zeta \gg 1$  is favored [7]. But it will significantly suppress the amplitude of GW. Thus in this article we just take  $\zeta$  to be merely a parameter, and suppose a situation that the dark glueball is not the main component of dark matter, or not the dark matter candidate at all. Such a setup justifies our treatment later, while the case  $\zeta \gg 1$  will be commented in the discussion section. Anyway, in what follows we will use  $T$  only, and the SM-sector temperature is simply  $\zeta T$ .

We use the Mathematica program AnyBubble [43] to numerically solve Eq. (37), and evaluate  $S_3(T)/T$  and the bubble nucleation rate  $\Gamma(T)$  in Eq.(35). The criterion for bubble nucleation is that at the nucleation temperature  $T_n$ , a single bubble is nucleated within one Hubble horizon volume; it roughly amounts to the condition  $\Gamma(T_n) \sim H(T_n)$ . In the radiation dominated universe, this condition reads  $S_3(T_n)/T_n \sim 140$ , and see Ref. [44] for more detailed discussions. Through this equation we determine the bubble nucleation temperature  $T_n$ .

With the bounce action and  $T_n$  at hand, we can calculate two key parameters characterizing the FOPT, which almost completely determine the GW spectra. One is the  $\alpha$  parameter, which measures the strength of the FOPT via the ratio between the latent heat and the total energy density of the universe at  $T = T_n$ ,

$$\alpha \equiv \frac{L_N(T_n)}{\rho_{\text{SM}}(\zeta T_n) + \rho_{\text{PYM}}(T_n)}, \quad (39)$$

The other one is  $\tilde{\beta}$ , the inverse time scale of PT duration in terms of the Hubble time scale,

$$\tilde{\beta} \equiv -\frac{1}{H} \frac{d}{dt} \left( \frac{S_3(T)}{T} \right) \bigg|_{t=t_n}, \quad (40)$$

with  $t_n$  the cosmic time corresponding to  $T_n$ . It is convenient to replace  $t$  with  $T$ , via the relation  $\frac{dt}{dT} = \frac{-1}{HT}$ , and then  $\tilde{\beta}$  goes like

$$\tilde{\beta} = T_n \frac{d}{dT} \left( \frac{S_3(T)}{T} \right) \bigg|_{T=T_n} \quad (41)$$

Now, both  $\alpha$  and  $\beta$  are calculated as a function of the dark- PYM sector temperature  $T$  (given certain  $\zeta$ ). The resultant numbers for the parameters relevant to the GW spectra are give in Table II. We see that the typical  $\tilde{\beta}$  is as huge as  $10^5$ , namely a very fast PT. That short duration of PT suppresses the production of GW. This result turns out to be fairly irrespective to whether  $\zeta$  is zero or nonzero (See Figs.5 and 7, and related discussions around there).

Let us end up with this subsection by stressing an interesting observation of  $\tilde{\beta}$ . That is, it shows a minimum at some color number  $N_m$ . This feature has been pointed out in [33, 52], but we would like to stress that the value of  $N_m$  depends on the model. For the model in Ref. [52],  $N_m = 6$ , while  $N_m = 4$  in Ref. [33] which adopts a very different model, the matrix model. In our model, we find that  $N_m = 7(9)$  for the 4 – 6(8) PLM; see Table. II.

The above feature may be partially understood. We can prove that  $\tilde{\beta}$  decreases with  $N$  in the large  $N$  region. In the sufficiently large  $N$  region, Eq. (37) can be solved once and for all, due to the scaling behavior of the effective potential  $V_N = N^2 U$  with  $U$  independent on  $N$ . We assume that temperature is fixed and thus drop its dependence. Denote the bounce solution for the potential  $U$  is  $\phi(R)$ , then the bounce solution for  $V_N$  is simply given by  $\phi_N(R) = \phi(NR)$ . With this solution, the three-dimensional Euclidean action  $S_3$  for  $N$  color can be rewritten in the form of

$$S_3 = \frac{2\pi}{N} \int_0^\infty r^2 dr \left[ \frac{1}{2} \left( \frac{d\phi}{dr} \right)^2 + U \right], \quad (42)$$

where both  $\phi$  and  $U$  have no dependence on  $N$  and therefore we obtain the scaling behavior of the action,  $S_3 \propto 1/N$ . For our discussions,  $T_n$  is always very close to  $T_c$ , which is determined by  $U$  thus universal to the large  $N$ . Hence, the nucleation condition  $S_3/T_n \simeq 140$  leads to a slightly larger  $T_n$  when increasing  $N$ . Moreover, the slope of  $S_3/T$  sharply increases when the temperature approaches  $T_c$ . Therefore,  $\tilde{\beta}$ , which is proportional to the slope, increases with  $N$ . Eventually, combining with the fact (not proved, just a numerical observation) that  $\tilde{\beta}$  decreases with  $N$  in the small  $N$  region, we obtain the conclusion that  $\tilde{\beta}$  reaches the minimum at some moderately large  $N$ .

Model and $N$	4-6 PLM $N = 4_1$	4-6 PLM $N = 4_2$	4-6 PLM $N = 5$	4-6 PLM $N = 6$	4-6 PLM $N = 7$	4-6 PLM $N = 8$	4-8 PLM $N = 4_1$
$T_c/g_*$	100 GeV /133	100 GeV /133	100 GeV /142	100 GeV /153	100 GeV /166	100 GeV /181	100 GeV /133
$T_n$	$0.9968T_c$	$0.9973T_c$	$0.9960T_c$	$0.9956T_c$	$0.9954T_c$	$0.9957T_c$	$0.9981T_c$
$\alpha$	0.094	0.095	0.160	0.229	0.300	0.363	0.095
$\tilde{\beta}$	97089	111073	75306	67404	64897	68694	159536
4-8 PLM $N = 4_2$	4-8 PLM $N = 5$	4-8 PLM $N = 6$	4-8 PLM $N = 7$	4-8 PLM $N = 8$	4-8 PLM $N = 9$	4-8 PLM $N = 10$	4-8 PLM $N = 11$
100 GeV /133	100 GeV /142	100 GeV /153	100 GeV /166	100 GeV /181	100 GeV /198	100 GeV /217	217 GeV /238
$0.9973T_c$	$0.9962T_c$	$0.9951T_c$	$0.9942T_c$	$0.9932T_c$	$0.9931T_c$	$0.9932T_c$	$0.9933T_c$
0.095	0.160	0.229	0.299	0.367	0.394	0.494	0.550
111497	80040	61638	51869	43684	43204	43240	43657

TABLE II: The reference values for the parameters relevant to the GW spectra, predicted from the 4-6 and 4-8 PLMs with  $N = 4 - 8$ , and  $N = 4 - 11$ , respectively. The subscript attached on 4 of  $N = 4$  denotes the same category as introduced in Table I. The SM contribution parameter  $\zeta$  has been set to 1.

### B. GW sources from the fast PT

In the cosmic FOPT, there are three kinds of sources for GWs, i.e., bubble collision, sound wave and magnetohydrodynamic (MHD) turbulence. The latent heat released during the FOPT distributes into these sources, but the fractions are not precisely determined yet. Usually, it is believed that the fraction of the latent heat transferred to the bubble collision is negligible,  $\kappa_{col} \ll 1$ , provided that  $\alpha$  does not become extremely large [45]. The GW sources are dominated by the two bulk motions of the plasma.

One bulk motion is the sound wave propagating in the plasma after the percolation, and the latent heat that goes into it is estimated to be [46]

$$\kappa_{sw} \approx \alpha(0.73 + 0.083\sqrt{\alpha} + \alpha)^{-1}, \quad (43)$$

suppressed by the small  $\alpha$ . The GW peak frequency at  $T_n$  is  $f_{sw,*} = 2(8\pi)^{1/3}/[\sqrt{3}(v_w - c_s)R_*]$  with  $R_*$  being the average bubble separation at the collision and the speed of sound in the plasma  $c_s = 1/\sqrt{3}$ . This separation is related to the typical time scale of PT via  $R_* = (8\pi)^{1/3}v_w/\beta_n$ , given the exponential approximation of  $\Gamma(T)$  around  $T_n$ . The observed GW spectra peak at  $f_{sw} = f_{sw,*}a_0/a(T_n)$ , as a result of redshift from the GW production time  $t_n$  to today; then the peak frequency is parameterized as [45]

$$\begin{aligned} f_{sw} &= 1.65 \times 10^{-5} \left( \frac{T_n}{100\text{GeV}} \right) \left( \frac{g_*}{100} \right)^{\frac{1}{6}} \frac{3.4}{(v_w - c_s)H_*R_*} \text{Hz} \\ &= 2.75 \times 10^{-5} \frac{\tilde{\beta}}{v_w} \left( \frac{T_n}{100\text{GeV}} \right) \left( \frac{g_*}{100} \right)^{\frac{1}{6}} \text{Hz}. \end{aligned} \quad (44)$$

The amplitude of the GW spectrum for the sound wave is then given by [45, 47]

$$h^2\Omega_{sw}(f) = 6.35 \times 10^{-6} (H_*R_*) (H_*\tau_{sw}) \left( \frac{\kappa_{sw}\alpha}{1+\alpha} \right)^2 \left( \frac{100}{g_*} \right)^{\frac{1}{3}} v_w S_{sw}(f), \quad (45)$$

where the shape of the spectrum takes the form of

$$S_{sw}(f) = (f/f_{sw})^3 \left[ \frac{7}{4 + 3(f/f_{sw})^2} \right]^{\frac{7}{2}}. \quad (46)$$

The amplitude is proportional to  $\tau_{sw}$ , the duration of the sound wave source, defined as  $H_*\tau_{sw} = \min[1, H_*R_*/U_f]$  with  $U_f$  being the root-mean-square fluid velocity [48]

$$U_f \simeq \frac{\sqrt{3}}{2} \left( \frac{\alpha(1 - \kappa_{col})}{1 + \alpha(1 - \kappa_{col})} \kappa_{sw} \right)^{1/2}. \quad (47)$$

A smooth expression for  $H_*\tau_{sw}$  is derived in Ref. [50], and it simply reduces to  $H_*R_*/U_f$  in the limit  $H_*R_*/U_f \ll 1$ . This is true for almost all confinement-deconfinement PTs, which will generate huge  $\beta$ . Consequently, the sound wave source is considerably suppressed by such a factor. So, in this case, the GW from the sound wave becomes

$$h^2\Omega_{sw}(f) = 6.3 \times 10^{-5} \frac{1}{\tilde{\beta}^2} \left( \frac{\kappa_{sw}\alpha}{1+\alpha} \right)^2 \left( \frac{100}{g^*} \right)^{\frac{1}{3}} v_w^2 S_{sw}(f). \quad (48)$$

To maximize the amplitude, we take the bubble wall velocity  $v_w = 1$ . This is reasonable because the background field  $l$  does not interact with the SM particles, and therefore the bubble expanding seems not be hampered by the plasma and soon turns to be relativistic. We leave a comment on this simplification in the discussion section.

When the sound wave period ends and the fluid flow becomes non-linear, then the other fluid bulk motion, the MHD turbulence is generated. If the sound wave  $\tau_{sw}$  is relatively long, at least one Hubble time scale, then the MHD turbulence is suppressed, having an efficiency factor  $\kappa_{turb} \sim 0.05\kappa_{sw}$  [48]. However, as shown above,  $\tau_{sw} \ll 1/H^*$  and consequently  $\kappa_{turb}$  may be significantly enhanced. But the quantitative enhancement is unknown yet owing to the fact that a part of the fluid motion not consumed by the sound speed wave can convert into heat. Optimistically, we assume that all of the energy transfers to turbulence, giving rise to the GW spectrum [49],

$$h^2\Omega_{turb}(f) = 3.3 \times 10^{-4} \frac{1}{\tilde{\beta}} \left( 1 - \frac{2(8\pi)^{1/3}v_w}{\sqrt{3}\tilde{\beta}} \right) \left( \frac{\kappa_{sw}\alpha}{1+\alpha} \right)^{\frac{3}{2}} \left( \frac{100}{g} \right)^{\frac{1}{3}} v_w S_{turb}(f), \quad (49)$$

with the shape function

$$S_{turb}(f) = \frac{(f/f_{turb})^3}{[1 + (f/f_{turb})]^{\frac{11}{3}} (1 + 8\pi f/h)}. \quad (50)$$

which, compared to  $S_{sw}(f)$ , shows a moderately large suppression  $\sim \mathcal{O}(10)$  in the high frequency region. The peak frequency is similar to that of the sound wave source [45],

$$\begin{aligned} f_{turb} &= 1.65 \times 10^{-5} \left( \frac{T_n}{100\text{GeV}} \right) \left( \frac{g_*}{100} \right)^{\frac{1}{6}} \frac{3.9}{(v_w - c_s)H_*R_*} \text{Hz} \\ &= 3.15 \times 10^{-5} \frac{\tilde{\beta}}{v_w} \frac{T}{100\text{GeV}} \left( \frac{g}{100} \right)^{\frac{1}{6}} \text{Hz}. \end{aligned} \quad (51)$$

### C. Predicted GW spectra

Using the formulae above combined with the 4-6 PLM in the previous section, we plot the GW spectra predicted from the dark  $SU(N)$  PYM theory in Fig. 4 for  $N = 4$  marked as “4-6 PLM”, in comparison with the prospected GW interferometer sensitivities in the future (LISA [8, 9], BBO [10–14], DECIGO [14–16] and TianQin [17]). In the figure, as a reference, we set  $\zeta = 0$  (i.e. no SM contributions), which can ideally be realized in the large  $N$  limit. The critical temperature  $T_c$  for the confinement-deconfinement PT has been set to 270 MeV, just as a reference point inspired by the PYM limit for QCD <sup>7</sup>. In Fig. 4, we have also made comparison with the Haar-type PLM in Eq. (9) (labeled by “Haar-type”), though it is inconsistent with lattice data on thermodynamical quantities in terms of the large  $N$  scaling as well as the confinement-deconfinement criticality scaling in  $T$ . From Fig. 4 we see that the predicted GW signal from the  $N = 4$  4-6 PLM can have high sensitivity reach to be probed by the prospected BBO detector. Note also that the 4-6 PLM’s signal is significantly different and gets larger than the Haar-type PLM’s.

Varying the input  $T_c$  value, we also plot the predicted GW signals for  $N = 4$ , in Fig. 5. In the left panel, we have taken  $\zeta = 0$  as in Fig. 4, while in the right panel  $\zeta = 1$ . As clearly seen from the figure, different critical temperatures will only shift the peak frequencies of GW and hardly affect the peak amplitudes. We also find that the SM contribution give no significant contribution to the GW spectra from the dark PYM. In Fig. 6, similar plots with  $\zeta = 1$  have been displayed for  $N = 4, 5, 6$ .

In Fig. 7 we show the  $N = 4$  4-8 PLM prediction to the GW spectra without the SM term ( $\zeta = 0$ ). The left panel displays the two scenarios with  $a_2 = 0$ , i.e. the category  $N = 4_1$ , or with  $a_2 \neq 0$ , i.e. the category  $N = 4_2$ , while in

<sup>7</sup> In the literature [51]  $T_c$  was estimated for  $N = 3$  to be  $\sim 260$  MeV with a particular string tension size input.

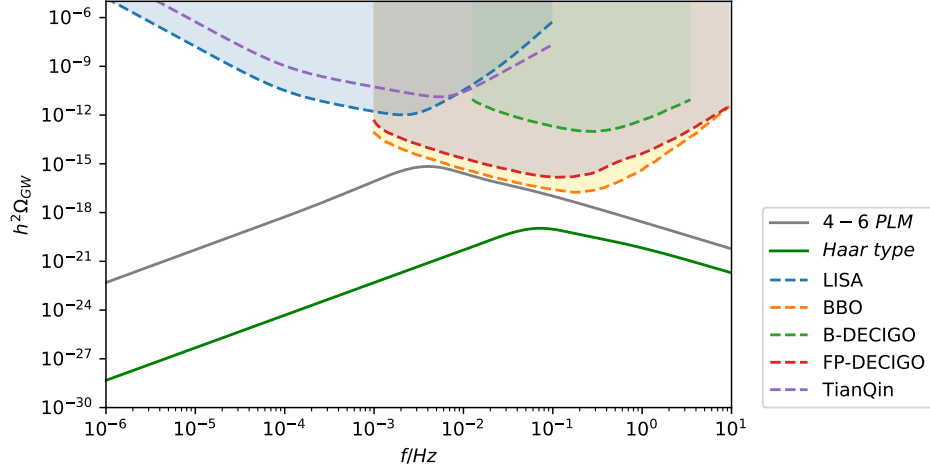


FIG. 4: GW spectra predicted from different models for  $N = 4$  under an extreme scenario that the secluded dark gluon plasma to highly dominate over the SM plasma (i.e.  $\zeta = 0$ ). The critical temperature has been set as  $T_c = 270$  MeV. For more details, see the text.

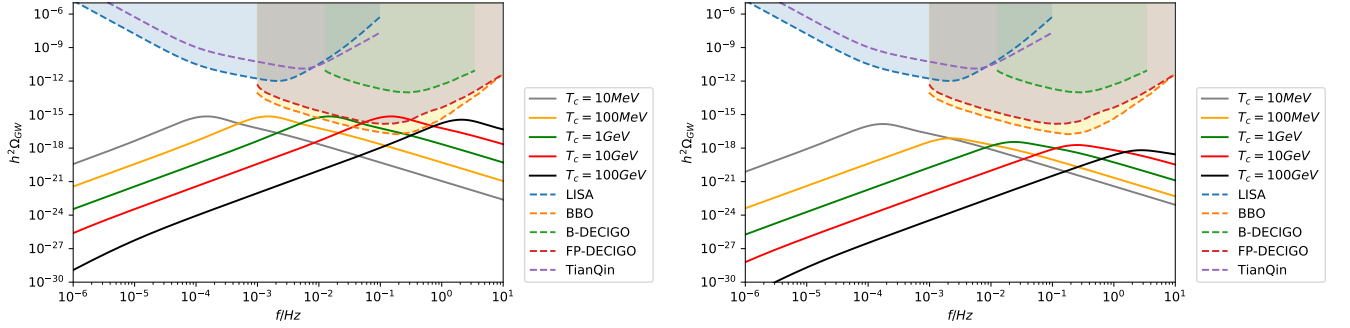


FIG. 5: GW spectra with the same condition as in Fig. 4, but with varying  $T_c$  in several orders. The right panel includes the SM contribution by  $\zeta = 1$ , while the left panel does not ( $\zeta = 0$ ).

the right panel, comparison between the 4-6 PLM and 4-8 PLM has been shown for the case with  $a_2 = 0$ , i.e. the category  $N = 4_1$ . In the figure we have taken  $\zeta = 0$  and  $T_c = 270$  MeV. We see that both 4-6 and 4-8 PLMs would be possible to be probed by BBO.

Taking larger  $N$ , the 4-8 PLM sensitivity gets larger and reach the maximum at  $N = 9$ , as expected from the minimum point of  $\tilde{\beta}$  in Table II. The left panel of Fig. 8 shows the predicted signals for  $N = 7, 8, 9$  with the SM contribution included ( $\zeta = 1$ ) and  $T_c = 10$  GeV fixed, and the right panel displays the  $T_c$  dependence for the  $N = 9$  signals. The figure implies that the GW spectra from the 4-8 PLM with larger  $N$  can be probed at earliest by BBO and DECIGO.

#### IV. CONCLUSION AND DISCUSSIONS

A pure  $SU(N)$  Yang-Mills (PYM) sector, for instance, predicted by the string theory, may be an active part of the particle physics beyond the standard model (SM). Maybe, such a PYM sector is completely secluded to the SM sector, and then we should peek into this dark sector by means of its gravitational wave (GW) signals, which are generated during the first-order (FO) confinement-deconfinement phase transition (PT).

The gauge invariant object, the Polyakov loop  $L$ , associated with the global  $Z_N$  symmetry of  $SU(N)$ , is a well defined order parameter of this PT. And a proper effective model based on  $L$ , namely the Polyakov loop model (PLM), is necessary to describe the confinement-deconfinement PT. In this article we have investigated the widely used Haar-type PLMs, and demonstrated that they fail to produce the large  $N$  scaling for the thermodynamical quantities and the latent heat at around the criticality of the PT reported from the lattice simulations. We then proposed a couple of

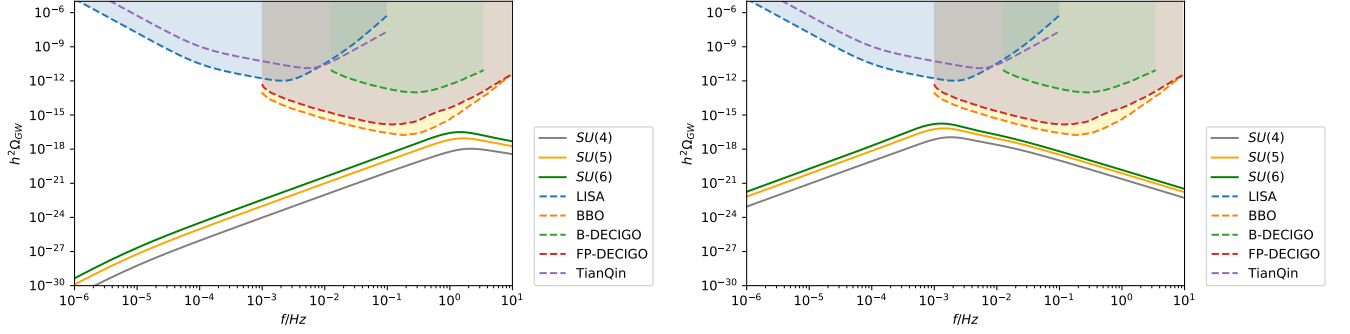


FIG. 6: GW signals from the 4-6 PLM for  $N = 4, 5, 6$  with  $T_c = 100$  GeV (left panel) and  $T_c = 100$  MeV (right panel). The SM contribution has been set as  $\zeta = 1$ . The signals with  $N = 7, 8$  for 4 – 6 PLMs will look like nearly overlapping with the  $N = 6$  signal in this plot, because of close  $\beta_s$  as read off from Table II.

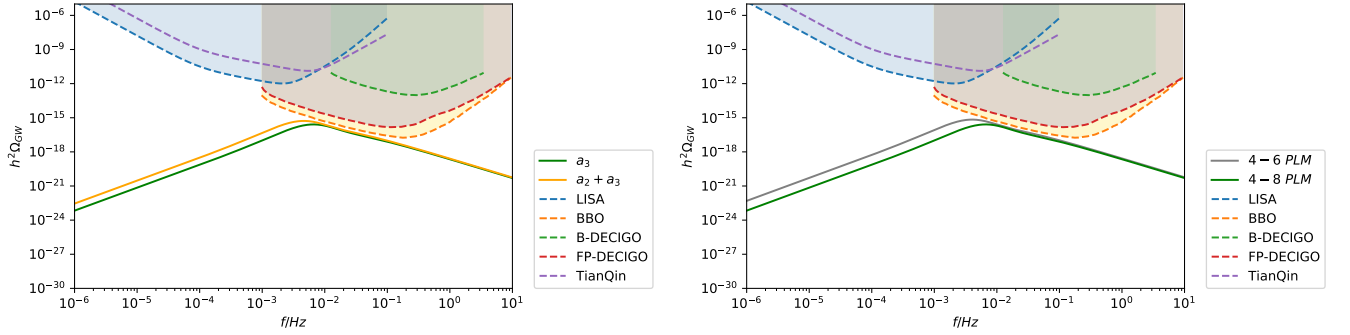


FIG. 7: Left panel: GW signals from 4-8 PLMs with  $a_2 = 0$  (labelled by “ $a_3$ ”, corresponding to the category  $N = 4_1$ ) and  $a_2 \neq 0$  (labelled by “ $a_2 + a_3$ ”, corresponding to the category  $N = 4_2$ ), corresponding to the fitting results in Fig.3, for  $N = 4$  with  $T_c = 270$  MeV. Right panel: Comparison of the GW signals from the 4-6 PLM and 4-8 PLM with  $a_2 = 0$ , for  $N = 4$  and  $T_c = 270$  MeV. The SM contribution has been turned off by taking  $\zeta = 0$ .

PLMs with polynomial terms, which was dubbed the 4-6 PLM and 4-8 PLM, with a negative quartic term to trigger the FOPT. Such a structure may naturally arise in the presence of a heavy PL with the center charge 2, given that the basic/normal PL having charge 1. We showed that those models give the consistent thermodynamical and large  $N$  properties at around the criticality. The predicted GW spectra were shown to have high enough sensitivity to be probed in the future prospected interferometers such as BBO and DECIGO

The dark PYM opens novel interesting possibilities in the early universe, and here are some open questions need to be addressed elsewhere:

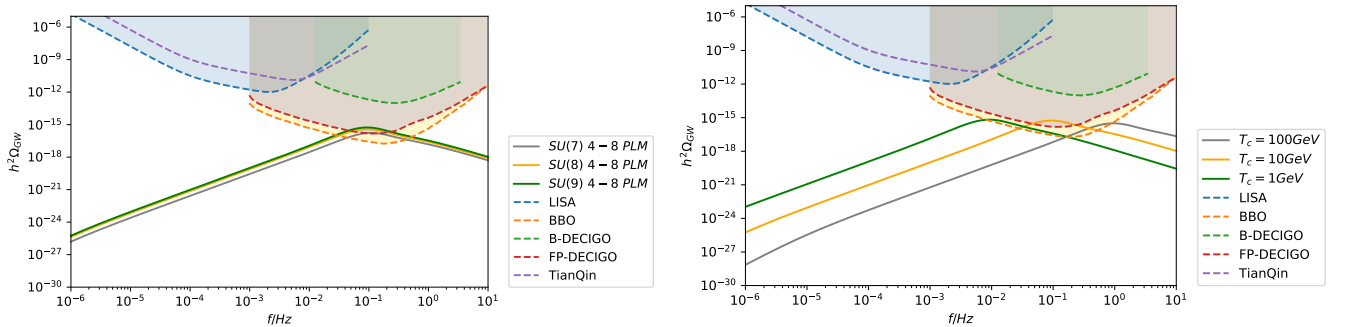


FIG. 8: Left panel: GW signals of 4 – 8 PLM PTs with  $N = 7, 8, 9$  at  $T_c = 10$  GeV. Right panel: The dependence of the critical temperature  $T_c$  on the GW signals from the  $N = 9$  4-8 PLM. Both panels have taken into account the SM contribution ( $\zeta = 1$ ).



- In discussing the bubble velocity, in Sec.III, we have argued that the bubble is expanding relativistically. Because the SM plasma does not provide friction with the bubble, it effectively is expanding in the vacuum, tracking the runaway behavior. However, the dark gluonic plasma is not empty, and we may should consider the quasi particle picture.
- The universe may experience a stage of PYM dominance. In this scenario, the dark glueball has a relatively short lifetime, decaying away before the onset of BBN due to the proper higher dimensional operators linking the two sectors.
- As can be read off from Table II, the parameter  $\tilde{\beta}$  decreases with the number of color  $N$ , implying that the PT in our models tends to happen more slowly, as  $N$  gets larger. This tendency is still operative even starting from  $N = 3$ . This dumping  $\tilde{\beta}$  in  $N$  is a characteristic feature of our PLM, which is compared to the PT nature predicted from the matrix model [33] exhibiting a growing scaling of the  $\tilde{\beta}$  in  $N$  for  $N > 4$ , but a dumping for  $N < 4$ . At  $N = 4$  the parameters  $\alpha$  and  $\tilde{\beta}$  have the same order of magnitude for both the matrix model and ours, so both models coincide at this  $N = 4$  and GW signals do as well. As one can see from Fig. 6, the peak strength of GW gets smaller as  $N$  decreases, hence it will be impossible to detect for  $N = 3$  by the prospected detectors. Thus the GW detection for the larger  $N$  signals would be a good discriminator between the matrix model and ours, where the latter's signals will be much stronger because of the much slower FOPTs. More detailed analysis along this line would be worth persisting.

Note added:

During the completion of this work, Ref. [52] has been posted and discussed GW signals from dark  $SU(N)$  PYM theory, also based on the PYM model with a Polynomial potential which includes all terms up to  $|l|^8$ . But we adopt a different strategy, considering the Polynomial potential merely including the 4-6 or 4-8 terms, motivated by the possible origin from integrating out a heavy PL with a higher center charge. We provide comparison between the two types of models. This point including the possible derivation of the 4-6 PLM has not been addressed in the literature. Besides, our work shows that the PLMs with the Haar measure term are incompatible with the large  $N$  scaling for the thermodynamical quantities and the latent heat.

### Acknowledgements

We thank Bo Feng and Ruiwen Ouyang for useful discussions, and are grateful to Huaikuo Guo and Zhi-Wei Wang for useful comments. This work is supported in part by the National Science Foundation of China (11775086) and the National Key Research and Development Program of China Grant No.2020YFC2201504 (ZK). S.M. work was supported in part by the National Science Foundation of China (NSFC) under Grant No.11747308, 11975108, 12047569 and the Seeds Funding of Jilin University.

- 
- [1] S. Nussinov, Phys. Lett. B 165, 55 (1985).
  - [2] S. M. Barr, R. S. Chivukula and E. Farhi, Phys. Lett. B 241, 387 (1990).
  - [3] P. Ko, N. Nagata and Y. Tang, Phys. Lett. B **773**, 513 (2017).
  - [4] H. An, S. L. Chen, R. N. Mohapatra and Y. Zhang, JHEP 1003, 124 (2010).
  - [5] Z. Chacko, H. S. Goh and R. Harnik, Phys. Rev. Lett. 96, 231802 (2006).
  - [6] R. Blumenhagen, M. Cvetič, P. Langacker and G. Shiu, Ann. Rev. Nucl. Part. Sci. 55, 71 (2005).
  - [7] Z. Kang, Phys. Lett. B **801**, 135149 (2020).
  - [8] P. Amaro-Seoane *et al.* [LISA], [arXiv:1702.00786 [astro-ph.IM]].
  - [9] J. Baker, J. Bellovary, P. L. Bender, E. Berti, R. Caldwell, J. Camp, J. W. Conklin, N. Cornish, C. Cutler and R. DeRosa, *et al.* [arXiv:1907.06482 [astro-ph.IM]].
  - [10] J. Crowder and N. J. Cornish, Phys. Rev. D **72**, 083005 (2005) doi:10.1103/PhysRevD.72.083005 [arXiv:gr-qc/0506015 [gr-qc]].
  - [11] V. Corbin and N. J. Cornish, Class. Quant. Grav. **23**, 2435-2446 (2006) doi:10.1088/0264-9381/23/7/014 [arXiv:gr-qc/0512039 [gr-qc]].
  - [12] G. M. Harry, P. Fritschel, D. A. Shaddock, W. Folkner and E. S. Phinney, Class. Quant. Grav. **23**, 4887-4894 (2006) [erratum: Class. Quant. Grav. **23**, 7361 (2006)] doi:10.1088/0264-9381/23/15/008
  - [13] E. Thrane and J. D. Romano, Phys. Rev. D **88**, no.12, 124032 (2013) doi:10.1103/PhysRevD.88.124032 [arXiv:1310.5300 [astro-ph.IM]].
  - [14] K. Yagi and N. Seto, Phys. Rev. D **83**, 044011 (2011) [erratum: Phys. Rev. D **95**, no.10, 109901 (2017)] doi:10.1103/PhysRevD.83.044011 [arXiv:1101.3940 [astro-ph.CO]].
  - [15] N. Seto, S. Kawamura and T. Nakamura, Phys. Rev. Lett. **87**, 221103 (2001) doi:10.1103/PhysRevLett.87.221103 [arXiv:astro-ph/0108011 [astro-ph]].

- [16] S. Isoyama, H. Nakano and T. Nakamura, PTEP **2018**, no.7, 073E01 (2018) doi:10.1093/ptep/pty078 [arXiv:1802.06977 [gr-qc]].
- [17] Y. Lu, Y. Gong, Z. Yi and F. Zhang, JCAP **12**, 031 (2019) doi:10.1088/1475-7516/2019/12/031 [arXiv:1907.11896 [gr-qc]]. from cosmological phase transitions, JCAP 1604 (2016) 001, [1512.06239].
- [18] B. Lucini, M. Teper and U. Wenger, JHEP **01**, 061 (2004) M. Panero, Phys.Rev.Lett. 103, 232001 (2009); S. Datta and S. Gupta, Phys.Rev. D82, 114505 (2010); B. Lucini, A. Rago, and E. Rinaldi, (2012), arXiv:1202.6684 [hep-lat].
- [19] P. N. Meisinger, T. R. Miller, and M. C. Ogilvie, Phys.Rev. D65, 034009 (2002).
- [20] A. Dumitru, Y. Guo, Y. Hidaka, C. P. K. Altes and R. D. Pisarski, Phys. Rev. D **86**, 105017 (2012)
- [21] R. D. Pisarski, Phys.Rev. D74, 121703 (2006).
- [22] T. Umeda, S. Ejiri, S. Aoki, T. Hatsuda, K. Kanaya, et al., Phys.Rev. D79, 051501 (2009).
- [23] S. Borsanyi, G. Endrodi, Z. Fodor, S. D. Katz and K. K. Szabo, JHEP **07**, 056 (2012).
- [24] A. M. Polyakov, Phys. Lett. B72 (1978) 477–480.
- [25] M. Panero, Phys.Rev.Lett. 103, 232001 (2009).
- [26] S. Datta and S. Gupta, Phys.Rev. D82, 114505 (2010).
- [27] N. Weiss, Phys. Rev. D24 (1981) 475; N. Weiss, Phys. Rev. D25 (1982) 2667.
- [28] K. Fukushima, Phys. Lett. B591, 277 (2004), hep-ph/0310121.
- [29] J. Kubo and M. Yamada, JHEP **10**, 003 (2018).
- [30] A. Dumitru, Y. Guo, Y. Hidaka, C. P. K. Altes and R. D. Pisarski, Phys. Rev. D **86**, 105017 (2012)
- [31] P. M. Lo, B. Friman, O. Kaczmarek, K. Redlich, and C. Sasaki, Physical Review D, vol. 88, Oct 2013.
- [32] A. Dumitru and R. D. Pisarski, Phys. Lett. B **525**, 95-100 (2002).
- [33] J. Halverson, C. Long, A. Maiti, B. Nelson and G. Salinas, [arXiv:2012.04071 [hep-ph]].
- [34] R. D. Pisarski, Nucl. Phys. A **702**, 151-158 (2002).
- [35] J. Braun, H. Gies and J. M. Pawłowski, Phys. Lett. B **684**, 262-267 (2010).
- [36] J. M. Pawłowski, D. F. Litim, S. Nedelko, and L. von Smekal, Phys. Rev. Lett. 93 (2004) 152002.
- [37] B. Svetitsky and L. G. Yaffe, Nucl. Phys. B210 (1982) 423.
- [38] R. D. Pisarski, Phys. Rev. D **62**, 111501 (2000) doi:10.1103/PhysRevD.62.111501 [arXiv:hep-ph/0006205 [hep-ph]].
- [39] K. Fukushima, Phys. Rev. D77, 114028 (2008), [Erratum: Phys. Rev.D78,039902(2008)], 0803.3318.
- [40] S. Roessner, C. Ratti, and W. Weise, Phys. Rev. D75 (2007) 034007.
- [41] S. Datta and S. Gupta, Phys. Rev. D **82**, 114505 (2010) doi:10.1103/PhysRevD.82.114505 [arXiv:1006.0938 [hep-lat]].
- [42] C. Ratti, M. A. Thaler and W. Weise, Phys. Rev. D **73**, 014019 (2006).
- [43] A. Masoumi, K. D. Olum and J. M. Wachter, JCAP **10**, 022 (2017) doi:10.1088/1475-7516/2017/10/022 [arXiv:1702.00356 [gr-qc]].
- [44] Z. Kang and J. Zhu, Phys. Rev. D **102**, no.5, 053011 (2020).
- [45] J. Ellis, M. Lewicki, J. M. No and V. Vaskonen, JCAP **1906**, 024 (2019).
- [46] J. R. Espinosa, T. Konstandin, J. M. No and G. Servant, JCAP 1006 (2010) 028.
- [47] C. Caprini, M. Chala, G. C. Dorsch, M. Hindmarsh, S. J. Huber, T. Konstandin, J. Kozaczuk, G. Nardini, J. M. No, K. Rummukainen, P. Schwaller, G. Servant, A. Tranberg and D. J. Weir, JCAP **03**, 024 (2020)
- [48] M. Hindmarsh, S. J. Huber, K. Rummukainen and D. J. Weir, Phys. Rev. D92 (2015) 123009, [1504.03291].
- [49] C. Caprini, R. Durrer and G. Servant, JCAP **12** (2009), 024
- [50] H. K. Guo, K. Sinha, D. Vagie and G. White, JCAP **01**, 001 (2021).
- [51] G. Boyd, J. Engels, F. Karsch, E. Laermann, C. Legeland, M. Lutgemeier and B. Petersson, Nucl. Phys. B **469**, 419-444 (1996) doi:10.1016/0550-3213(96)00170-8 [arXiv:hep-lat/9602007 [hep-lat]].
- [52] W. C. Huang, M. Reichert, F. Sannino and Z. W. Wang, [arXiv:2012.11614 [hep-ph]].